

Structural and functional analysis of hydroxynitrile lyase from *Baliospermum montanum* with crystal structure, molecular dynamics and enzyme kinetics[☆]

Shogo Nakano¹, Mohammad Dadashipour¹, Yasuhisa Asano^{*}

Biotechnology Research Center and Department of Biotechnology, Toyama Prefectural University, 5180 Kurokawa, Imizu, Toyama 939-0398, Japan
Asano Active Enzyme Molecule Project, ERATO, JST, 5180 Kurokawa, Imizu, Toyama 939-0398, Japan

ARTICLE INFO

Article history:

Received 15 July 2014

Received in revised form 1 September 2014

Accepted 4 September 2014

Available online 16 September 2014

Keywords:

Hydroxynitrile lyase

High benzyl affinity

Broad substrate specificity

Crystal structure

Molecular dynamics simulation

Enzyme kinetics

ABSTRACT

Hydroxynitrile lyases (HNLs) catalyze degradation of cyanohydrins to hydrogen cyanide and the corresponding ketone or aldehyde. HNLs can also catalyze the reverse reaction, i.e., synthesis of cyanohydrins. Although several crystal structures of *S*-selective hydroxynitrile lyases (*S*-HNLs) have been reported, it remains unknown whether and how dynamics at the active site of *S*-HNLs influence their broad substrate specificity and affinity. In this study, we analyzed the structure, dynamics and function of *S*-HNL from *Baliospermum montanum* (*BmHNL*), which has an α/β hydrolase fold. Two crystal structures of *BmHNL*, apo1 and apo2, were determined at 2.55 and 1.9 Å, respectively. Structural comparison between *BmHNL* (apo2) and *S*-HNL from *Hevea brasiliensis* with (*S*)-mandelonitrile bound to the active site revealed that hydrophobic residues at the entrance region of *BmHNL* formed hydrophobic interactions with the benzene ring of the substrate. The flexible structures of these hydrophobic residues were confirmed by a 15 ns molecular dynamics simulation. This flexibility regulated the size of the active site cavity, enabling binding of various substrates to *BmHNL*. The high affinity of *BmHNL* toward substrates containing a benzene ring was also confirmed by comparing the kinetics of *BmHNL* and *S*-HNL from *Manihot esculenta*. Taken together, the results indicated that the flexibility and placement of the residues are important for the broad substrate specificity of *S*-HNLs.

© 2014 Elsevier B.V. All rights reserved.

1. Introduction

Cyanogenesis is a process by which plants defend themselves against predators or infecting microorganisms by generating hydrogen cyanide (HCN). In vivo, hydroxynitrile lyases (HNLs) catalyze the final reaction in the aldoxime–nitrile pathway, resulting in the release of HCN and a ketone or aldehyde from the corresponding cyanohydrin (Fig. 1). Although there are about 3000 cyanogenic plant species [1], to date only a few plant HNLs have been purified and precisely characterized [2]. HNLs are categorized as *R*- or *S*-selective enzymes, based on their cyanohydrin substrates [3,4]. In industry, these enzymes are also

used as stable biocatalysts in the synthesis of cyanohydrins, which are widely used as precursors for various chemical compounds [5–9]. In this study, we focused on *S*-selective hydroxynitrile lyases (*S*-HNLs).

S-HNLs with an α/β hydrolase fold (lipase–esterase superfamily) (EC 4.1.2.47) have been found in cassava (*MeHNL*), tropical rubber tree (*HbHNL*), and another member of the Euphorbiaceae, *Baliospermum montanum* (*BmHNL*) [10,11]. These *S*-HNLs share more than 50% amino acid identity and have broad substrate specificity. The active site of *S*-HNLs is formed by a hydrogen bond interaction among the catalytic triad (Ser–His–Asp), a lysine residue, and other hydrophobic residues (Table 1) [12–16]. The roles of the catalytic residues have been investigated by various methods including high resolution crystallography [12], enzyme kinetic analyses, and quantum mechanical (QM) calculations [12,17]. The *S*-HNLs have been proposed to act via a concerted proton-transfer mechanism in which the catalytic serine residue abstracts the hydrogen atom from the substrate's hydroxyl group, and then produces a cyanide ion to obtain a hydrogen atom from the catalytic lysine residue [12,17].

Although the reaction mechanism of *S*-HNLs has been extensively analyzed, less attention has been paid to the functions of the hydrophobic residues, with the exception of Trp128, whose side chain influences the stereoselectivity of *MeHNL* [18]. Elucidation of the hydrophobic residues' function is necessary in order to perform rational design of

Abbreviations: HNL, hydroxynitrile lyase; *S*-HNL, *S*-selective hydroxynitrile lyase; (*R*)-Man, (*R*)-mandelonitrile; (*S*)-Man, (*S*)-mandelonitrile; *rac*-Man, *racemic* mandelonitrile; MD, molecular dynamics; RMSD, root mean square deviation; RMSF, root mean square fluctuation; *MeHNL*, *S*-selective hydroxynitrile lyase from *Manihot esculenta*; *HbHNL*, *S*-selective hydroxynitrile lyase from *Hevea brasiliensis*; *BmHNL*, *S*-selective hydroxynitrile lyase from *Baliospermum montanum*; *AtHNL*, *R*-selective hydroxynitrile lyase from *Arabidopsis thaliana*

[☆] This research was supported by ERATO Asano Active Enzyme Molecule Project, Japan Science and Technology Agency (JST).

^{*} Corresponding author at: Biotechnology Research Center and Department of Biotechnology, Toyama Prefectural University, 5180 Kurokawa, Imizu, Toyama 939-0398, Japan. Tel.: +81 766 56 7500x530; fax: +81 766 56 2498.

E-mail address: asano@pu-toyama.ac.jp (Y. Asano).

¹ These authors contributed equally to this work.

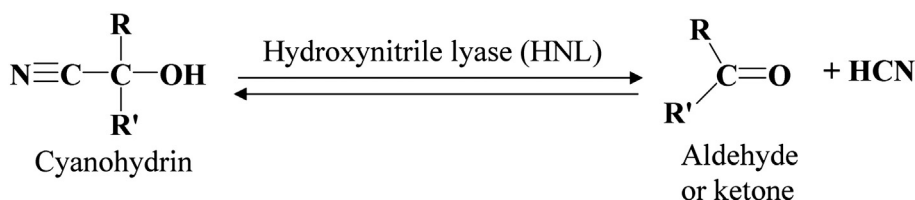


Fig. 1. Reaction catalyzed by hydroxynitrile lyase (HNL). The enzyme catalyzes both degradation (forward reaction) and synthesis (reverse reaction) of cyanohydrins, which are important intermediates in organic synthesis and biocatalysis.

S-HNLs, e.g., to improve substrate specificity and stereoselectivity. Furthermore, because it was suggested that the hydrophobic residues play an important role in recognizing various substrates and introducing cyanide ion into the active site [12], functional analysis of these hydrophobic residues should lead to an explanation of the broad substrate specificity of the enzyme. Based on a model structure of *BmHNL* [10], the hydrophobic residues of *BmHNL* are predicted to differ from those of *MeHNL* and *HbHNL* (Table 1). Thus, *BmHNL* is expected to have different enzymatic characteristics than the other two S-HNLs. Structural and biochemical analyses of *BmHNL* would help elucidating the role of these hydrophobic residues.

In this study, we determined two crystal structures of *BmHNL*. Structural analysis of *BmHNL* suggested that hydrophobic residues at the active site form hydrophobic interactions with the substrate, and molecular dynamics (MD) simulation indicated that the hydrophobic residues near the entrance region have flexible side chains. Steady-state kinetic parameters of *BmHNL* and *MeHNL* were determined, using various aromatic substrates, revealing that *BmHNL* can form a more stable Michaelis complex than *MeHNL* with substrates containing benzene rings. Taken together, our findings suggest that dynamical structural changes may occur in these proteins in solution. Alterations in the placements of residues may explain the differences in the functions and substrate specificities of various S-HNLs.

2. Materials & methods

2.1. Preparation and purification of recombinant S-HNLs

BmHNL was produced using a transformant of *Escherichia coli* BL21 (DE3) strain harboring a previously constructed plasmid, pColBM1 [10], which contains the *bmhnl* gene. Briefly, 45 L of Luria-Bertani (LB) broth containing ampicillin (final concentration of 50 $\mu\text{g mL}^{-1}$) was inoculated with a pre-culture (grown at 37 °C to $\text{OD}_{600} = 1$) of the aforementioned transformant. After inoculation of the cells for 10 h at 37 °C at an agitation rate of 200 rpm, the cultures were subjected to cold shock for 2 h at 4 °C, and then transferred into a shaking incubator pre-adjusted to 18 °C. Gene expression was induced with 0.5 mM (final concentration) isopropyl β -D-1-thiogalactopyranoside (IPTG). The overnight cultures were harvested, and the cells were lysed by sonication (Insonator 201 M, Kubota, Japan). *BmHNL* was purified from a cleared cell-free extract by single-step affinity chromatography using Ni-Sephrose Fast Flow (GE Healthcare, Stockholm, Sweden). Purified *BmHNL* was dialyzed against 20 mM potassium phosphate buffer (KPB) pH 7.0. The protein sequence contains an N-terminal fusion of

20 amino acids, including a 6 \times His tag; the tagged enzyme was used for both kinetics and crystallography. Recombinant *MeHNL* was purified to homogeneity as described previously [11].

2.2. Crystallization and structure determination

Purified *BmHNL* was concentrated to 15–35 mg mL^{-1} using Amicon Ultra 0.5 mL centrifugal filters (EMD Millipore Corporation, Billerica, MA, USA). Screening for optimal crystallization conditions was performed at 20 °C using the sitting drop vapor diffusion method. Drops were prepared by mixing 2.0 μL of protein solution with 1.0 μL of reservoir solution. Screening was performed using CrystalScreen 1-1 (Hampton Research, CA, USA). Thin and plate like crystals (apo1) appeared after 1 month in 30% 2-methyl-2, 4-pentanediol (MPD), 0.1 M sodium acetic acid (pH 4.6) and 0.02 M CaCl_2 . Using CrystalScreen 2-15 (Hampton Research), cubic like crystals (apo2) appeared after 1 week: 1.0 M lithium sulfate, 0.1 M sodium citrate (pH 5.6), and 0.5 M ammonium sulfate.

The apo1 crystal was directly mounted and flash-cooled under a liquid nitrogen stream (100 K). Diffraction data was collected in-house using a Rigaku Micro-Max007 $\text{CuK}\alpha$ rotating-anode X-ray generator and a Rigaku R-AXISVII image-plate detector. X-ray diffraction data from the apo2 crystal was collected at BL-17A (KEK, Tsukuba) under a liquid nitrogen stream. The apo2 crystal was soaked quickly in a reservoir containing 20% ethylene glycol. For both apo1 and apo2 data, indexing and integration of the diffraction data and scaling were performed using HKL2000 and Scalepack [19], respectively. Initial phase was determined by Molrep [20] in the CCP4 program suite [21] using the crystal structure of *MeHNL* (PDB ID: 1 EB8) as a template. Model building and structure refinement were performed using Coot [22] and Refmac [23], respectively. All structural figures were prepared by PyMol [24]. Crystallographic parameters are shown in Table 2.

2.3. Molecular dynamics simulation of *BmHNL*

Chains A and B of the *BmHNL* (apo2) structure were used as the initial model for MD simulation. Initially, protonation of the structure was performed, and then TIP3P water molecules were solvated into the box ($11 \times 12 \times 12 \text{ nm}^3$) at a solvent density of 1.0 g cm^{-3} using the software package MOE2011 [25]. Energy minimization was performed using the Charmm27 force field by applying constraint to the catalytic triad residues (Ser80, Asp207 and His235) of *BmHNL*. The total charge of the system was calculated using a custom-made Python script, and then sodium ions (Na^+) or chloride ions (Cl^-) were placed in the system to neutralize its charge.

All MD simulations were performed using NAMD 2.9 software [26] with periodic boundary conditions. Electrostatic interactions among the atoms were estimated by the standard particle mesh Ewald method [27]. All hydrogen atoms were constrained, and the RATTLE algorithm [28] was applied to the calculation. Simulation time step was 2 fs. The temperature was set to 300 K during the calculation, and a Langevin thermostat was applied. The isothermal–isobaric (NPT) ensemble was applied at a pressure of 1.0 bar.

The simulated annealing process was applied as described previously [29]. During the annealing process, the catalytic triad was constrained.

Table 1
The hydrophobic residues located in the active site of the three S-HNLs.

Residue number ^a	81	121	122	128	133	146	152	157	178
<i>MeHNL</i>	Cys	<i>Leu</i> ^c	<i>Leu</i>	Trp	Tyr ^b	<i>Met</i>	Leu	Leu	<i>Leu</i>
<i>HbHNL</i>	Cys	<i>Leu</i>	<i>Met</i>	Trp	Tyr ^b	<i>Leu</i>	Leu	Leu	<i>Leu</i>
<i>BmHNL</i>	Gly	Phe ^b	<i>Ser</i>	Trp	Phe ^b	<i>Val</i>	Thr	Ile	Phe ^b

^a The number corresponds to residue number of *BmHNL*.

^b Aromatic residues are shown in bold.

^c The residues located in the entrance region (Fig. 2C) are shown in italics.

Download English Version:

<https://daneshyari.com/en/article/7560774>

Download Persian Version:

<https://daneshyari.com/article/7560774>

[Daneshyari.com](https://daneshyari.com)